

Long-Term Safety and Tolerability of *BMP7* and *HGF* Gene Overexpression in Rabbit Cornea

Suneel Gupta^{1,2}, Nishant R. Sinha^{1,2}, Lynn M. Martin^{1,2}, Landon M. Keele^{1,2}, Prashant R. Sinha^{1,2}, Jason T. Rodier³, James R. Landreneau^{1,3}, Nathan P. Hesemann^{1,3}, and Rajiv R. Mohan¹⁻³

¹ Harry S. Truman Memorial Veterans' Hospital, Columbia, MO, USA

² One-Health Vision Research Program, Departments of Ophthalmology and Biomedical Sciences, College of Veterinary Medicine, University of Missouri, Columbia, MO, USA

³ Mason Eye Institute, School of Medicine, University of Missouri, Columbia, MO, USA

Correspondence: Rajiv R. Mohan, Professor of Ophthalmology and Molecular Medicine, University of Missouri, 1600 East Rollins Street, Columbia, MO 65211, USA.
e-mail: mohanr@health.missouri.edu

Received: February 21, 2021

Accepted: July 18, 2021

Published: August 12, 2021

Keywords: BMP7; HGF; corneal fibrosis; gene therapy

Citation: Gupta S, Sinha NR, Martin LM, Keele LM, Sinha PR, Rodier JT, Landreneau JR, Hesemann NP, Mohan RR. Long-term safety and tolerability of *BMP7* and *HGF* gene overexpression in rabbit cornea. *Transl Vis Sci Technol.* 2021;10(10):6. <https://doi.org/10.1167/tvst.10.10.6>

Purpose: Tissue-targeted localized *BMP7+HGF* genes delivered into the stroma via nanoparticle effectively treats corneal fibrosis and rehabilitates transparency *in vivo* without acute toxicity. This study evaluated the long-term safety and tolerability of *BMP7+HGF* nanomedicine for the eye *in vivo*.

Methods: One eye each of 36 rabbits received balanced salt solution (group 1, naïve; $n = 12$), naked vector with polyethylenimine-conjugated gold nanoparticles (PEI2-GNP; group 2, naked-vector; $n = 12$), or *BMP7+HGF* genes with PEI2-GNP (group 3, *BMP7+HGF*; $n = 12$) via a topical delivery technique. Safety and tolerability measurements were performed by clinical biomicroscopy in live rabbits at predetermined time intervals up to 7 months. Corneal tissues were collected at 2 months and 7 months after treatment and subjected to histology, immunofluorescence, and quantitative real-time PCR analyses.

Results: Clinical ophthalmic examinations and modified MacDonalD-Shadduck scores showed no significant changes in corneal thickness ($P = 0.3389$), tear flow ($P = 0.2121$), intraocular pressure ($P = 0.9958$), epithelial abrasion, or ocular abnormality. Slit-lamp, stereo, confocal, and specular biomicroscopy showed no signs of blepharospasm chemosis, erythema, epiphora, abnormal ocular discharge, or changes in epithelium, stroma, and endothelium after *BMP7+HGF* therapy for up to 7 months, as compared with control groups. Throughout the 7-month period, no significant changes were recorded in endothelial density ($P = 0.9581$). Histological and molecular data were well corroborated with the subjective clinical analyses and showed no differences in the naïve, naked-vector, and *BMP7+HGF* groups.

Conclusions: Localized *BMP7+HGF* therapy is a safe, tolerable, and innovative modality for the treatment of corneal fibrosis.

Translational Relevance: Nanoparticle-mediated *BMP7+HGF* combination gene therapy has the potential to treat corneal fibrosis *in vivo* without short- or long-term toxicity.

Introduction

Corneal fibrosis and scar formation due to traumatic, chemical, and surgical insults are common causes of visual disability. Such corneal disorders are the third leading cause of global blindness and

affect around 1.3 million Americans every year.¹⁻³ Several co-morbidities are associated with corneal fibrosis, including inflammation, neovascularization, and elevated intraocular pressure.⁴⁻⁶ Although decades of research regarding fibrosis have helped elucidate the underlying mechanisms, safe and tolerable non-surgical treatments are currently limited. According

to the National Center for Advancing Translational Sciences, only 500 human diseases are treatable with an estimated 10,000 drugs available to date, which underscores the necessity to develop new drugs and treatment options.⁷ Pharmacological therapy and corneal transplant surgery are currently the treatment of choice in fibrotic disorders but have numerous side effects.^{8–10}

Gene therapy has shown encouraging preclinical results for various disorders; however, safety, tolerability, and technical concerns have restricted its successful translation into clinical therapy. In the eye, the cornea is well suited for gene therapy due to its ease of accessibility and immune-privileged environment. Corneal tissue allows topical instillation of gene delivery vectors and visual monitoring of the genes packaged within vectors.^{11–14} The chances of systemic exposure from topical gene therapy in corneal tissue are minimal. The success of the gene therapy is dependent on the safety and efficacy of the delivered genes and the carrier vector in the targeted tissue. Proof-of-concept for gene therapies has been established in several experimental models. In the last three decades, several studies from our group and others have shown the efficacy of gene therapy in ocular tissues using various viral and non-viral vectors.^{15–19} Such therapies include inhibition of corneal fibrosis and neovascularization.^{20–24} Despite clinical and preclinical efficacy studies, we still lack evidence to precisely assess the long-term safety and efficacy of clinical gene therapy.²⁵

The transforming growth factor-beta (TGF β) cytokine superfamily activates fibrosis cascades via Smad signaling.²⁶ In the past, we have successfully demonstrated the role of bone morphogenic protein 7 (BMP7) in the regulation of TGF β /Smad signaling, and it is therefore a potential therapeutic target for the treatment of corneal haze.²² In addition to BMP7, we have shown that injury to the corneal epithelium upregulates hepatocyte growth factor (HGF) and modulates corneal wound healing.²⁷ The importance of *BMP7* and *HGF* genes in corneal fibrosis has been well characterized in animal models.²⁴ One major component of translational research in gene therapy is detailing its short- and long-term safety and tolerability. To the best of our knowledge, no studies have been conducted to test the long-term safety and tolerability of *BMP7* and *HGF* combination gene therapy in corneal tissue. This study aimed to establish the long-term safety and tolerability of polyethylenimine-conjugated gold nanoparticles (PEI2-GNP)-(BMP7+HGF) gene therapy in corneal tissue at the clinical, histological, and molecular levels for a translational perspective.

Materials and Methods

Chemicals and Supplies

Artificial tears (Rugby Laboratories, Livonia, MI) and sterile Weck-Cel ophthalmic spears (BVI Medical, Waltham, MA) were purchased from Thermo Fisher Scientific (Grand Island, NY). Surgical forceps, wire Speculum, and Westcott scissors were purchased from World Precision Instruments (Sarasota, FL). Ketamine hydrochloride (JHP Pharmaceuticals, Rochester, MI), xylazine hydrochloride (XylaMed; Bimeda, Oakbrook Terrace, IL), pentobarbital sodium and phenytoin sodium (Euthasol; Virbac AH, Westlake, TX), and topical 0.5% proparacaine hydrochloride (Alcon, Fort Worth, TX) were obtained from the pharmacy of the Harry S. Truman Memorial Veterans' Hospital (Columbia, MO). Hematoxylin and eosin (H&E) solutions were procured from StatLab Medical Products (McKinney, TX). Balanced salt solution, 2-methyl butane, and antifade mounting medium with 4',6-diamidino-2-phenylindole dihydrochloride (DAPI; Vector Laboratories, Burlingame, CA) were obtained from Thermo Fisher Scientific.

Animals

The Institutional Animal Care and Use Committees of the Harry S. Truman Memorial Veterans' Hospital and the University of Missouri approved the study. Animals were treated in accordance with the ARVO Statement for the Use of Animals in Ophthalmic and Vision Research. Thirty-six New Zealand White rabbits between 4 and 5 pounds in weight were procured from Charles River Laboratories (Wilmington, MA). Both male and female rabbits were used and were selected randomly for each group to avoid potential sex-based variability. Rabbits were housed in temperature-controlled (21°C \pm 1°C) rooms with a 12-hour light/12-hour dark cycle and were provided ad libitum access to food and water. Rabbits were anesthetized with an intramuscular injection of a ketamine hydrochloride (50 mg/kg) and xylazine hydrochloride (10 mg/kg) cocktail. Each rabbit received one drop of topical anesthetic, proparacaine hydrochloride (0.5%), onto the eye prior to gene delivery and clinical evaluations to minimize pain and discomfort. Only one eye of each animal was used for the study. Animals were divided into three groups. The corneas of group 1 received balanced salt solution (naïve; $n = 12$), group 2 received naked vector with PEI2-GNP (naked-vector; $n = 12$), and group 3 received *BMP7* and *HGF* genes with PEI2-GNP (*BMP7+HGF*; $n = 12$) via a customized reported

technique.³ Rabbits were thermally supported throughout the procedure and during the anesthetic recovery period.

Generation and Transduction of PEI2-GNP-(BMP7+HGF) Genes

PEI2-GNPs were synthesized as reported previously.²⁸ The transfection solution of PEI2-GNP with corresponding genes was prepared similarly as reported earlier.²⁴ In brief, the PEI2-GNPs were mixed with plasmid at a nitrogen-to-phosphate ratio of 180 by stirring 37.5 μ L of 150-mM PEI2-GNPs with 10 μ g plasmid DNA (pTRUF11 expressing the *BMP7* or *HGF* gene under control of hybrid cytomegalovirus chicken β -actin promoter), with 10% glucose (weight/volume), and were brought to a total volume of 100 μ L. The PEI2-GNP solution was incubated at 37°C for 30 minutes prior to application onto the cornea. One eye of each animal received transfection solution topically for 5 minutes with the help of a cloning cylinder, as reported earlier.¹²

Clinical and Live Biomicroscopic Evaluations

The clinical eye evaluation and biomicroscopic eye imaging procedures in live rabbits were performed under general anesthesia before transfection and at the predetermined intervals (30 minutes, 1 day, 3 days, 7 days, 14 days, 21 days, 1 month, 2 months, 3 months, 5 months, and 7 months) after gene delivery.

Slit-Lamp Biomicroscopic Examinations

Slit-lamp narrow- and wide-beam evaluations were performed in rabbit eyes for clinical assessment. A slit-lamp biomicroscope (SL-15 portable slit-lamp; Kowa Optimed, Tokyo, Japan) coupled with a high-definition, portable digital imaging system (VK-2, version 5.50; Kowa Optimed) was used to record the clinical ocular examination. A stereomicroscope (MZ16F; Leica Microsystems, Wetzlar, Germany) equipped with a digital camera (SpotCam RT KE; Diagnostic Instruments, Sterling Heights, MI) was used to assess eye health following our reported protocol.²⁴ All *in vivo* clinical exams of the cornea and anterior chamber were performed by at least two investigators (SG, LMM, JTR, or NPH) in a masked manner. To prevent corneal desiccation, eyes were kept moist with artificial tears during the microscopic examinations.

Fluorescein Eye Stain Test for Assessment of Corneal Epithelial Health

Corneal epithelial defects were observed by applying a commercial ophthalmic fluorescein stain (Altafluor Benox; Altaire Pharmaceuticals, Riverhead, NY). Epithelial defects were viewed under a cobalt light blue filter and recorded under a green fluorescent protein light filter using a slit-lamp microscope equipped with an image-capturing system (Leica MZ16F) and the SpotCam RT KE digital camera following our reported protocol.³ These clinical photographs were scored by a minimum of two independent investigators (SG, LMM, JTR, JRL, or NPH) in a masked fashion.

Assessment of Corneal Inflammation, Intraocular Pressure, and Tear Flow

For quantification of corneal edema, an ultrasonic pachymeter (AccuPach VI Pachymeter; Accutome, Malvern, PA) was used to assess central corneal thickness before and after the PEI2-GNP-naked or PEI2-GNP-(*BMP7+HGF*) vectors. To determine the impact of gene therapy on aqueous humor regulation before and after gene delivery, intraocular pressure (IOP) measurement was evaluated using a handheld tonometer (Tono-Pen AVIA tonometer; Reichert, Depew, NY). All IOP measurements were performed between 9 AM and 11 AM to minimize normal diurnal variations in IOP. To account for changes in tear production, the volume of tears was computed with the help of Schirmer Tear Test Strips (Thermo Fisher Scientific) at each time point before and after the gene delivery in live animals. Tear production of each animal was recorded at the same time by one operator to avoid operator-based variations.

Ocular Health Evaluation by Modified MacDonald-Shadduck Score

To assess the safety and tolerability of PEI2-GNP-(*BMP7+HGF*) gene therapy, ocular examinations were scored following the modified MacDonald-Shadduck ocular scoring system.^{24,29} Briefly, scores were assigned based on corneal tissue evaluation (opacity, affected area, corneal neovascularization severity, and reepithelialization) and conjunctival tissue evaluation (congestion, chemosis, swelling, and discharge). Eye examinations were completed independently by at least two examiners (LMM, JTR, JRL, NPH, or SG) at selected times (before and 1, 3, and 7 months after gene transfer).

Confocal *In Vivo* Biomicroscopic Assessment

Confocal *in vivo* microscopy was used to capture corneal tissue images at the cellular level from different depths. The HRT3-RCM confocal imaging system (Heidelberg Engineering, Heidelberg, Germany) was used to record the images of each rabbit cornea starting from the epithelium and going to the endothelium layer as reported earlier.³⁰ A minimum of four confocal microscopy through-focus scans were performed in the central region of each cornea using a lens speed of 60 $\mu\text{m/s}$. Each scan had a step size between images of $\sim 2 \mu\text{m}$. The field of view for each 384×384 -pixel image was $400 \mu\text{m} \times 400 \mu\text{m}$, resulting in a voxel size of $1.04 \mu\text{m} \times 1.04 \mu\text{m} \times 2 \mu\text{m}$ (x, y, z).

Specular *In Vivo* Biomicroscopic Assessment

Corneal endothelial cell morphology and density are routinely used to gauge the safety of new drugs, devices, and therapeutic interventions during clinical trials. Thus, images of the corneal endothelium were captured for each eye with a non-contact specular microscope (NSP-9900; Konan Medical, Irvine, CA). The images were captured with magnification for reliable endothelial cell density determination and morphometric analysis. The fixed-frame method was used for the quantitative analysis of cell structure, coefficient of variation, and percentage of hexagonal cells.³¹

Euthanasia and Corneal Tissue Collection

Rabbits were humanely euthanized with an intravenous injection of Euthasol (150 mg/kg) while under general anesthesia at either 2 months ($n = 18$) or 7 months ($n = 18$) after gene transfer. A secondary euthanasia with Euthasol was also performed. Death of the animal was confirmed with cardiac auscultation. Corneas were collected with surgical forceps and Westcott scissors under an operating ophthalmology microscope (Leica Wild M690). The corneal tissues were immediately placed in molds containing optimal cutting temperature compound and snap frozen in a container of 2-methyl butane immersed in liquid nitrogen or directly placed into cryovials and dipped in liquid nitrogen. Frozen tissues were maintained at -80°C until further evaluation. Sections $8 \mu\text{m}$ thick were prepared with a cryomicrotome, mounted on glass microscopic slides, and preserved at -80°C for subsequent analysis. The cryovials with frozen corneal tissues were used for mRNA extraction and molecular analysis.

Histopathological Evaluations

H&E Staining

Naïve, naked-vector, and gene-delivered groups of rabbit corneal tissue sections were used for H&E staining to assess cellular morphological parameters. H&E staining was performed following a protocol reported previously.²⁴ Additionally, corneal sections were also sent to the Veterinary Medical Diagnostic Laboratory at the University of Missouri for histology examinations.

Masson's Trichrome Staining

Rabbit corneal tissue sections of all groups underwent Masson's trichrome staining to evaluate alterations in collagen, a key component of the extracellular matrix (ECM). Masson's trichrome staining was performed independently within our lab²⁴ and also by the Veterinary Medical Diagnostic Laboratory at the University of Missouri to enhance rigor.

DAPI Staining

DAPI immunostaining was used to visualize cellular density by analyzing DAPI-stained nuclei in corneal tissue sections prepared from control and gene-delivered animals under fluorescence microscope as reported earlier.³² In brief, frozen corneal tissue sections were left at room temperature for 15 minutes and then washed three times with $1 \times$ PBS for 5 minutes each time. Excess fluid from tissue sections was removed using Kimwipes, a drop of DAPI antifade VECTASHIELD medium (H1200; Vector Laboratories) was applied, and sections were mounted with premier coverslips. The stained sections were viewed and photographed with a Leica DM 4000B fluorescence microscope equipped with a SpotCam RT KE digital camera.

Inflammatory Cell Staining

To investigate the presence of an inflammatory response in corneal tissue after gene delivery, immunofluorescence staining was performed using M1/70 monoclonal antibody, which binds to CD11b, following a reported method.²⁴ In brief, corneal tissue sections were blocked with 2% bovine serum albumin at room temperature for 30 minutes, followed by incubation with primary rat anti-CD11b antibody (550282, 1:200 dilution; BD Biosciences, Franklin Lakes, NJ) for 90 minutes and with Alexa Fluor 594 Goat anti-Rat IgG (H+L) Cross-Adsorbed Secondary Antibody (A-11007, 1:1000 dilution; Invitrogen, Carlsbad, CA) for 60 minutes at room temperature. Thereafter, sections were copiously washed with PBS and mounted with DAPI antifade VECTASHIELD

Table 1. Sequence of Primers Used in the Study

Gene Name	Forward Primer (5'–3')	Reverse Primer (5'–3')	Accession No.
Primers Used for Relative qRT-PCR mRNA Expression Analysis			
Beta actin (<i>β-actin</i>)	CGGCTACAGCTTACCACCA	CAGGCAGCTCGTAGCTCTTC	X_00351
<i>α</i> -Smooth muscle actin (<i>α-SMA</i>)	TGGGTGACGAAGCACAGAGC	CTTCAGGGGCAACACGAAGC	NM_001613
Fibronectin (<i>FN</i>)	CGCAGCTTCGAGATCAGTGC	TCGACGGGATCACACTTCCA	NM_002026
Transforming growth factor-beta 1 (<i>TGFβ1</i>)	TCATACCACCTTCCGATTGCCCT	TGGATATGGCCTGACTCTTGCT	NM_001135599.1
Tumor necrosis factor alpha (<i>TNFα</i>)	CCCAGGCAGTCAGATCATCTTC	AGCTGCCCTCAGCTTGA	U42625.1
Cyclooxygenase 2 (<i>COX-2</i>)	GCCTGGTCTGATGATGATG	GTATTAGCCTGCTTGCTGG	AY462100.1
Nuclear factor kappa B (<i>NFκB</i>)	AGTGTGGAGTTCAGGATAAC	GAGAATGAAGGTGGATGATTGC	NM_001261403.3
Vascular endothelial growth factor (<i>VEGF</i>)	ACCCATGGCAGAAGAAGGAGACAA	ACTCCAGGCTTTCATCATTGCAGC	AF024710.1
Pigment epithelium-derived factor (<i>PEDF</i>)	TGATGTCGGACCTAAGGCTGTTT	ATGAATGAACCTCGGAGGTGAGGTC	NM_002615.4
Angiopoietin 1 (<i>ANGPT1</i>)	TTTGCTTTCCTCGTGCATTCTG	CACATTGCCCATGTTGAATCCGGT	NM_001146
Bone morphogenetic protein 7 (<i>BMP7</i>)	ACTCCTACATGAACGCCA	AAGTAGGACACAGAGATGCG	XM_002724263.1
Hepatocyte growth factor (<i>HGF</i>)	ATGTCAGCCCTGGAGTTCATGAT	AGCGTACCTCTGGATTGCTTGTA	NM_000601.4
Primers used for standard qRT-PCR gene copy number analysis			
Bone morphogenetic protein 7 (<i>BMP7</i>)	CTACTTCGACGACAGCTCTAATG	TCCTTGATGATGGCCATGTTAT	Custom oligos (plasmid DNA)
Hepatocyte growth factor (<i>HGF</i>)	TCTGTGACATTCTCAGTGTTTC	AGAGTTTTAGGGATAGGCTTAC	Custom oligos (plasmid DNA)

medium. The appropriate positive (frozen section of normal mouse spleen) and negative (irrelevant isotype-matched primary antibodies and use of primary or secondary antibody alone) controls were included in each immunostaining.

TUNEL Assay

The cellular toxicity from apoptotic death in corneas was determined with the terminal deoxynucleotidyl transferase dUTP nick-end labeling (TUNEL) assay (S7165, ApopTag Red In Situ Apoptosis Detection Kit; Serologicals Corporation, Norcross, GA) following the manufacturer's guidelines and as reported earlier.²⁴ This assay modifies DNA utilizing terminal deoxynucleotidyl transferase (TdT) to detect positive cells undergoing apoptosis. In brief, corneal tissue sections were fixed in 1% paraformaldehyde for 10 minutes. The fixed sections were washed with equilibration buffer and incubated with TdT enzyme solution for 1 hour at 37°C. The reaction was stopped by a stop buffer followed by a PBS rinse and incubated with anti-digoxigenin rhodamine antibody for 30 minutes at room temperature. The stained slides were mounted with VECTASHIELD antifade DAPI-containing medium. Rhodamine-conjugated apoptotic cells (red) and DAPI-stained nuclei (blue) were viewed and photographed with a Leica DMI4000B fluorescence microscope fitted with a SpotCam RT KE digital camera system.

Real-Time Quantitative Reverse Transcription PCR Analysis

The relative changes of mRNA levels in rabbit corneas at 2 months and 7 months after gene delivery were evaluated with real-time quantitative reverse transcription polymerase chain reaction (qRT-PCR) using the QuantStudio 6 Flex Real-Time PCR System

(Thermo Fisher Scientific). Total RNA was extracted from experimental rabbit corneal tissues using the RNeasy Mini Kit (Qiagen, Hilden, Germany). Then, 2 μg mRNA was used for cDNA conversion using a commercial reverse transcription system (Promega, Madison, WI) as reported earlier.²⁴ The changes in the mRNA expression of different inflammatory (*NFκB*, *TNFα*, and *COX-2*), fibrotic (*αSMA*, *FN*, and *TGFβ1*), and angiogenic (*VEGF*, *PEDF*, and *ANGPT1*) genes were studied. A 20-μL qPCR reaction mixture contained 2 μL of cDNA, 2 μL of 200-nM forward primer, 2 μL of 200-nM reverse primer, 10 μL of 2× SYBR green supermix (Bio-Rad Laboratories, Hercules, CA), and 4 μL of RNase/DNase free water. The qRT-PCR was run at universal cycle conditions, including initial denaturation at 95°C for 10 minutes and 40 cycles of denaturation at 95°C for 15 seconds, followed by annealing and extension at 60°C for 60 seconds. Beta-actin (*β-actin*) was used as a house-keeping gene. The relative mRNA expression was calculated using the $2^{-\Delta\Delta C_t}$ method and reported as relative fold change with respect to the corresponding control values. The details of primers used in the analysis are provided in Table 1.

Measurement of Gene Copies

The harvested corneas were pulverized in liquid nitrogen, and genomic DNA was isolated (Qiagen DNeasy kit). Real-time qPCR reactions were performed to determine the number of delivered copies of the *HGF* and *BMP7* genes in rabbit corneas following a protocol reported previously.²⁴ A 10-fold serial dilution of plasmid with the test gene (10^0 – 10^8 /μg DNA) was used for standard curves. The PCR reactions were run at 95°C for 10 minutes, 40 cycles at 95°C for 15 seconds, and 60°C for 60 seconds.

The nucleotide sequences of the forward and reverse primers used in analysis are provided in [Table 1](#).

Statistical Analysis

Statistical analysis was performed using Prism 6.07 (GraphPad, San Diego, CA). One-way analysis of variance (ANOVA) or two-way ANOVA with the Tukey or Bonferroni multiple comparison post hoc test was used depending on research design for all clinical data. $P < 0.05$ was considered statistically significant.

Results

Clinical Ophthalmic Examinations and Tests in Live Animals

The clinical ophthalmologic evaluations in rabbits at regular intervals until 7 months found no significant differences in eyes of the three groups (naïve, naked-vector, and *BMP7+HGF*). The periodic clinical evaluations suggested that over-expression of *BMP7* and *HGF* genes via nanoparticles was safe and tolerable to rabbit eyes *in vivo*. Slit-lamp narrow- and wide-beam examinations showed no signs of ocular inflammation, corneal haze, neovascularization, chemosis, or other ocular anomaly of the cornea, conjunctiva, or sclera after naked-vector or *BMP7+HGF* gene therapy

over a time-dependent progression for up to 7 months compared with naïve control ([Figs. 1, 2](#)).

The fluorescein eye test showed no signs of epithelial abnormality throughout the 7-month time period ([Fig. 3](#)). As expected, positive fluorescein stain in epithelium 30 minutes after gene delivery was observed in areas where epithelium was removed to facilitate gene transfer ([Fig. 3](#)).

Pachymetry, tonometry, and Schirmer test analyses did not find any statistically significant differences in the corneal thickness, IOP, or tear flow, respectively, in rabbit eyes for the 7 months evaluated after gene delivery. The corneal thickness ($P = 0.3389$), tear flow ($P = 0.2121$), and IOP ($P = 0.9958$) in rabbit eyes showed no significant deviation from naïve eyes and were in normal acceptable clinical range ([Fig. 4](#)). An expected, non-statistically significant alternation in the corneal thickness, tear volume per minute, and IOP was observed for the first 24 hours due to mild injury to the corneal epithelium which was a part of the minimally invasive gene transfer technique ([Fig. 4](#)).

In Vivo Confocal Biomicroscopy Evaluations

The HRT3-RCM confocal imaging system was used to gauge the morphology and health of rabbit corneal tissue from epithelium to endothelium. The confocal microscopy through-focus scans were taken en face of the cornea parallel to the epithelium surface. As evident

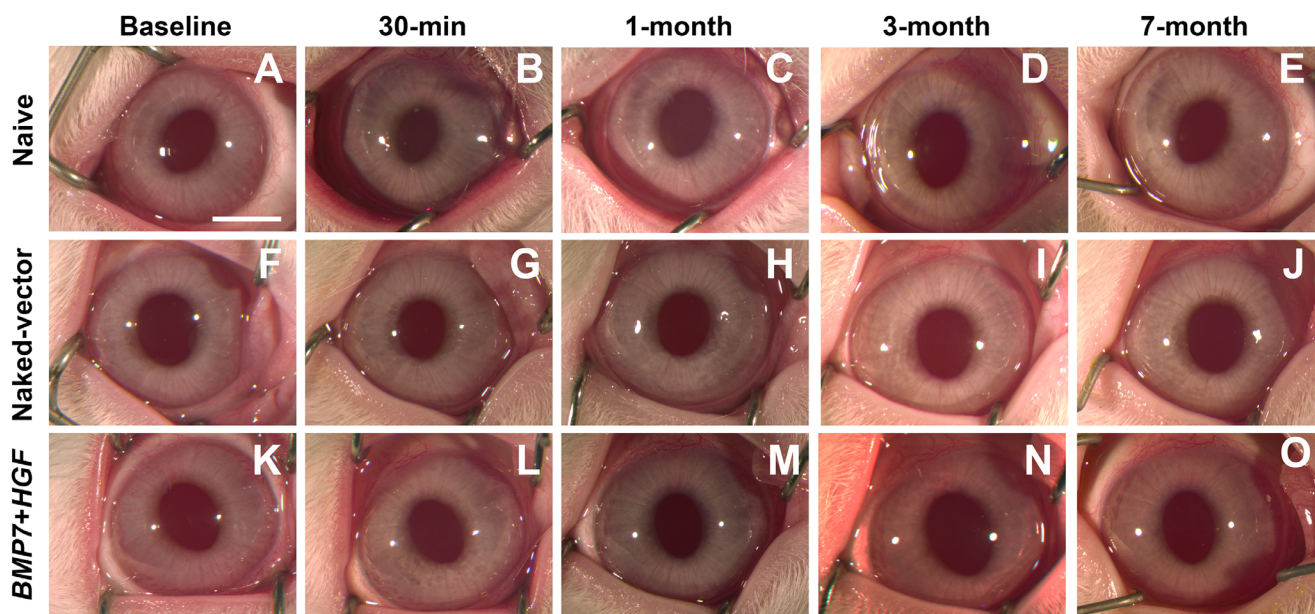


Figure 1. *In vivo* live stereo biomicroscopic images show the long-term (up to 7 months) safety and tolerability profiles of PEI2-GNP-(*BMP7+HGF*) gene therapy in the rabbit eyes. The images show no signs of adverse effects, including inflammation, opacity, or corneal neovascularization, in the *BMP7+HGF* group (K–O) as compared with the naïve (A–E) or naked-vector (F–J) control groups of animals. Scale bar: 2.0 mm.

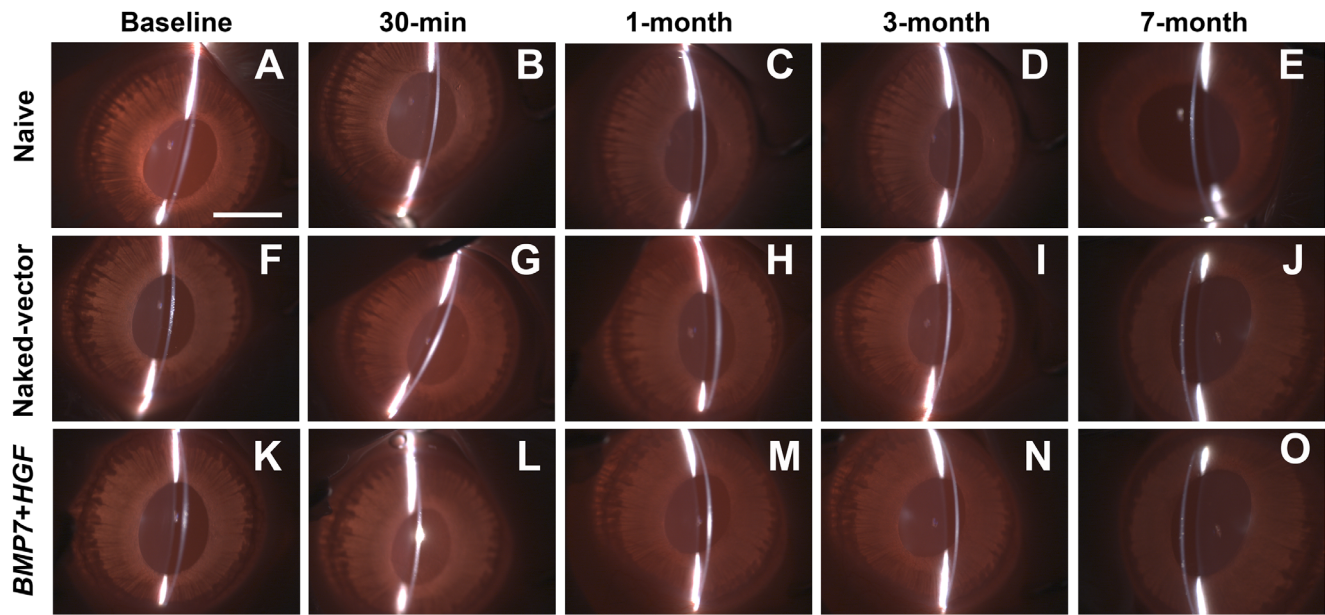


Figure 2. Representative slit-lamp, narrow-beam, *in vivo* live images indicating the long-term (up to 7 months) safety and tolerability of *BMP7+HGF* gene therapy in rabbit eyes. The slit-beam analysis showed no signs of inflammation or corneal opacity in the eye after *BMP7+HGF* gene therapy (K–O), and images were similar to those for the naïve (A–E) and naked-vector (F–J) control groups of animals. Scale bar: 2.0 mm.

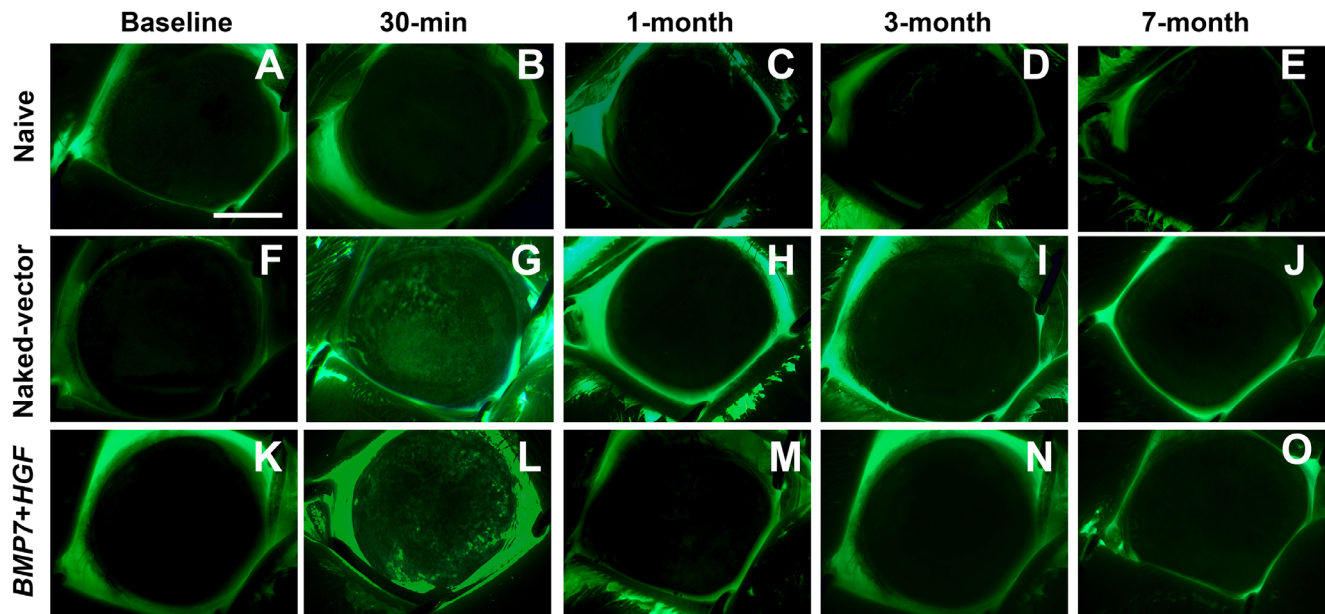


Figure 3. Representative fluorescein dye test images of rabbit eyes revealing corneal epithelial health progression after *BMP7+HGF* gene therapy up to 7 months. The fluorescein-stained images showed no signs of corneal abrasion or epithelial defects after *BMP7+HGF* gene therapy (K–O), and images were similar to those for the naïve (A–E) and naked-vector (F–J) control groups of animals. Scale bar: 2.0 mm

from the representative confocal images, no noticeable variation was detected in the shape or size of the superficial epithelial cells of rabbit corneal tissues of the *BMP7+HGF* gene therapy group compared with the naïve or naked-vector control groups (Fig. 5). The images of all three groups showed similar morphol-

ogy in each cell layer of rabbit cornea (Fig. 5). The superficial epithelial cells have a polygonal shape with a bright nucleus (Figs. 5A, 5G, 5M), the wing cells and basal epithelial cells appear with vivid cell borders and dark cytoplasm (Figs. 5B, 5H, 5N), the stromal layers— anterior (Figs. 5C, 5I, 5O), mid (Figs. 5D, 5J, 5P), and

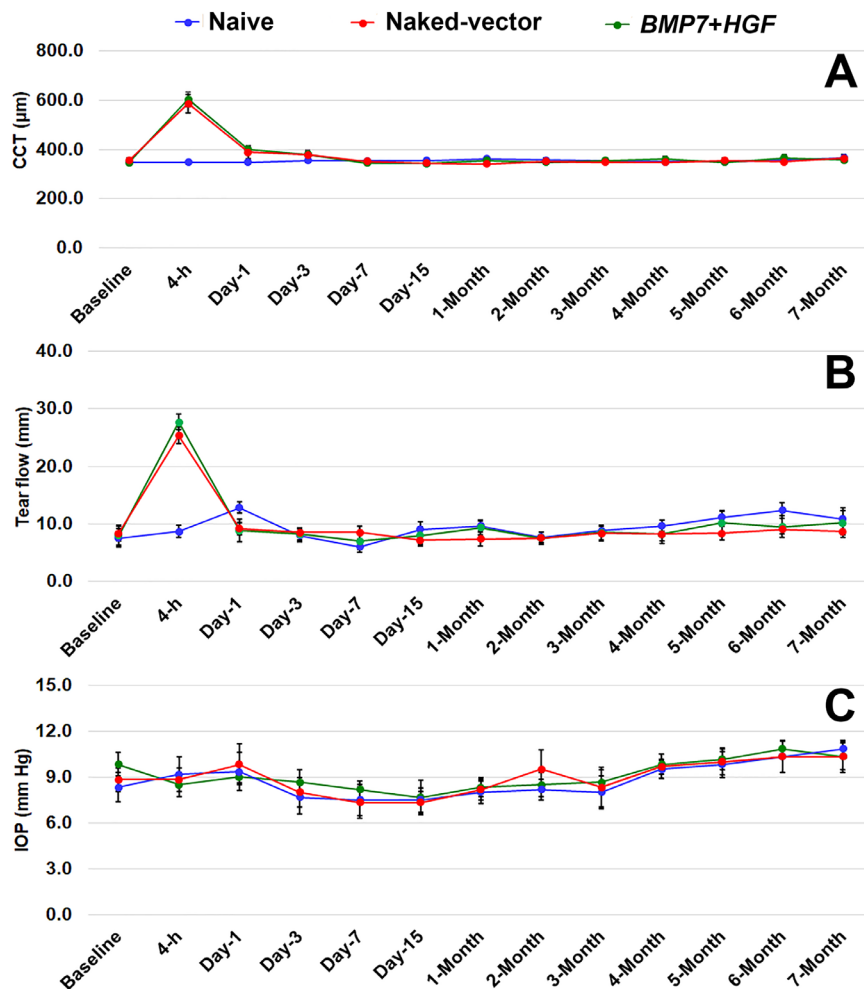


Figure 4. Line graphs show the safety and tolerability of *BMP7+HGF* gene therapy in rabbit eyes for up to 7 months. The topical *BMP7+HGF* gene therapy caused no changes in (A) central corneal thickness (CCT), (B) ocular tear flow, or (C) IOP. The measurements were similar to those for the naïve and naked-vector control group animals. Two-way ANOVA with Bonferroni post hoc test was used for multiple comparison, and $P > 0.05$ was considered non-significant in statistical analyses.

posterior (Figs. 5E, 5K, 5Q)—showed an organized keratocyte pattern with basal nerve plexuses, and the endothelial cells showed the characteristic hexagonal pattern (Figs. 5F, 5L, 5R). The keratocyte nuclei of the stromal cells were hyperreflective, and the reflectivity of the cytoplasm was a homogeneous pattern in all layers of the corneal tissue (Figs. 5C–5E, 5I–5K, 5O–5Q). The endothelial layer of all groups showed a normal hexagonal pattern and cell density (F, 5L, 5R).

In Vivo Specular Biomicroscopy Evaluations

Changes in endothelial cell morphology, density, and coefficient of variation were analyzed with specular biomicroscopy (Fig. 6). No significant changes were recorded in corneal endothelial cell density ($P = 0.9581$) (Fig. 6A), coefficient of variation ($P = 0.1256$)

(Fig. 6B), or hexagonality ($P = 0.7917$) (Fig. 6C) of the naïve, naked-vector, and *BMP7+HGF* gene-delivered rabbit eyes.

Modified MacDonald–Shadduck Score Evaluations

Modified MacDonald–Shadduck scores were assigned by two examiners in a masked manner in live rabbits. The cumulative scores presented in Table 2 revealed no significant differences ($P > 0.05$) in the eyes of all three groups (naïve, naked-vector, and *BMP7+HGF*). Also, no noticeable deviations appeared in the corneal clarity, pupillary light reflexes, erythema, chemosis, congestion, or discharge from the

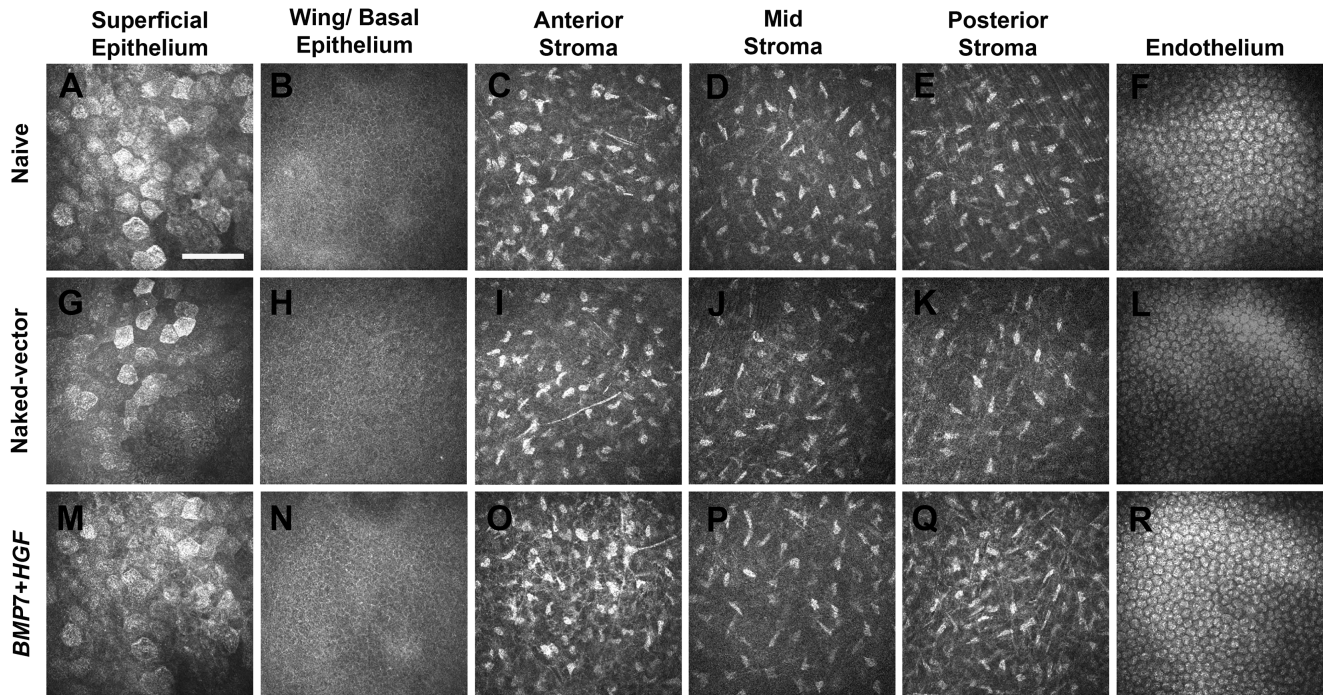


Figure 5. Representative *in vivo* confocal microscopy through-focus scans of all layers of the rabbit cornea tissue in the naïve (A–F), naked-vector (G–L), and *BMP7+HGF* (M–R) animal groups. Images were obtained with the HRT3-RCM confocal imaging system. The (M) epithelial superficial and (N) wing/basal cell layers; the (O) anterior, (P) mid-, and (Q) posterior stromal layers; and the (R) endothelial layers of the *BMP7+HGF* gene therapy group of eyes showed morphology and health similar to that of corresponding cells of the naïve (A–F) and naked-vector (G–L) control animals. Each image in the figure was captured from the central cornea and represented a varying relative depth to the front surface of the TomoCap. A speed of 60 $\mu\text{m/s}$ was used for the confocal microscopy through-focus scan in each group of animals. *Scale bar:* 100 μm

ocular tissues of naïve, naked-vector, and *BMP7+HGF* gene-delivered animals.

Histopathological Evaluations

H&E, Masson's Trichrome, and DAPI Staining

Histopathological evaluations of the naïve, naked-vector, and *BMP7+HGF* gene-delivered corneas harvested at 2 months and 7 months demonstrated similar findings in H&E staining, Masson's trichrome staining, and DAPI immunofluorescence; thus, only 7-month analysis data are presented. As evident from the H&E images, no appreciable morphologic changes were observed in *BMP7+HGF* gene therapy corneal tissue sections as compared with naïve and naked-vector control corneal tissue sections (Figs. 7A–7C).

Masson's trichrome staining was used to visualize collagenous connective tissue fibers in corneal sections. Collagen is an important component of the ECM of corneal tissues. The evaluations of Masson's trichrome-stained rabbit corneal tissue sections showed no considerable variations in gross collagen level as evident from the blue color staining level in the *BMP7+HGF* gene therapy group

compared with the naïve and naked-vector control groups (Figs. 7D–7F).

DAPI, an efficient nuclear staining reagent, was used to compare cellular density in corneal sections of the three experimental groups. The fluorescence quantification of DAPI-stained nuclei detected no significant differences in cellular density ($P = 0.8101$) of the naïve, naked-vector-delivered, or *BMP7+HGF*-delivered corneas (Figs. 7G–7I).

In Vivo Cytotoxicity and Inflammatory Responses

To evaluate the *in vivo* cytotoxicity and tolerability of *BMP7+HGF* gene therapy, we performed the TUNEL assay, which largely identifies apoptotic cells (Fig. 8). The TUNEL immunostaining did not find distinctive TUNEL+ cells in corneal tissues of naïve, naked-vector-delivered, and *BMP7+HGF*-delivered animals at 2 months and 7 months. The quantification of TUNEL+ cells in images depicted no significant cytotoxicity ($P = 0.7965$) to ocular tissue in eyes of any of the three groups at 7 months (Figs. 8A–8C). An expected, normal levels of TUNEL+ cells were noted in the corneal epithelium, which further illustrated that *BMP7+HGF* gene therapy did not compromise the normal turnover of the corneal epithelial cells in rabbit

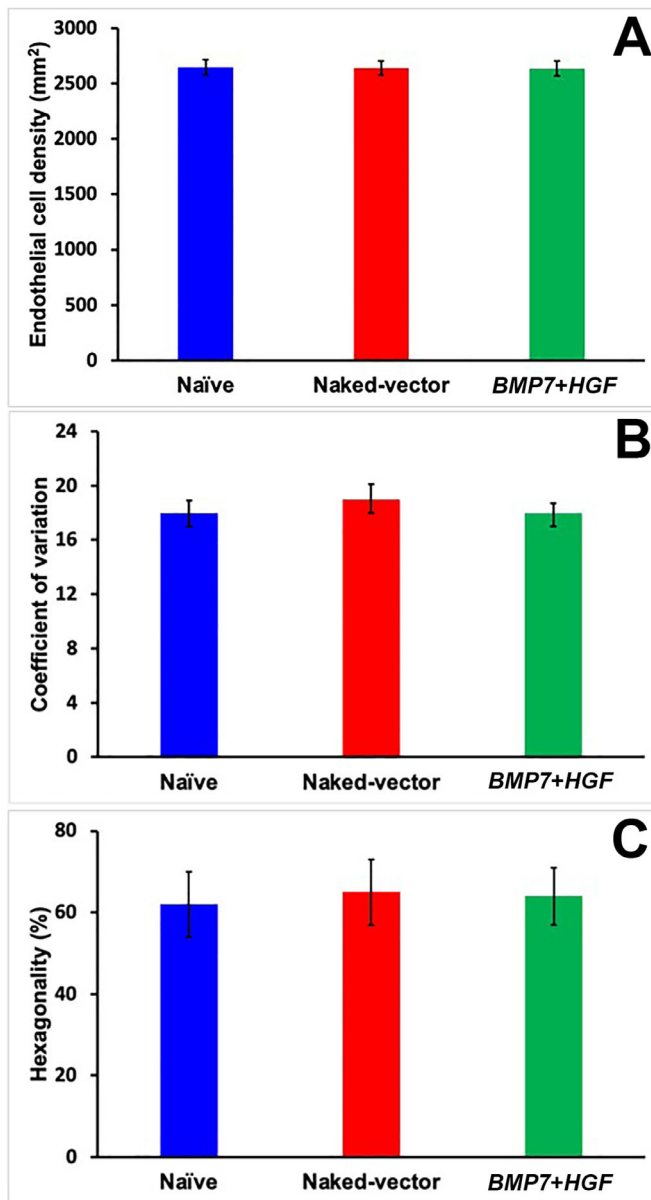


Figure 6. Bar graph showing cellular density, coefficient of variation, and hexagonality of corneal endothelial cells in rabbit eyes quantified with a clinical specular microscope. No significant changes in (A) corneal endothelial density, (B) coefficient of variation, or (C) hexagonality were observed among the eyes of the naïve, naked-vector, and *BMP7+HGF* animals, indicating that *BMP7+HGF* gene therapy is safe and tolerable in eyes *in vivo*. One-way ANOVA with Tukey post hoc test was used for multiple comparison, and $P > 0.05$ was considered non-significant in statistical analyses.

eyes *in vivo* (Figs. 8A–8C, arrows). Similar findings were noted in the analysis of corneal tissues at 2 months (data not shown). Overall, TUNEL analysis indicated that PEI2-GNP–(*BMP7+HGF*) gene therapy was not cytotoxic and was tolerable when applied to rabbit eyes.

To study the effects of *BMP7+HGF* gene therapy on immune response, CD11b immunostaining was performed. CD11b is expressed in many immune

cells, including monocytes/macrophages, neutrophils, eosinophils, basophils, and lymphoid cells.³³ The CD11b immunofluorescence showed no appearance of inflammatory cells in the rabbit corneas of naïve, naked-vector, or *BMP7+HGF* groups (Fig. 8). Quantification of CD11b+ cells in corneal sections of the *BMP7+HGF* group showed no significant deviations ($P = 0.6783$) in number from naïve or naked-vector control corneas at 7 months (Fig. 8D–8F, arrowheads). The corneal tissues at 2 months showed similar results (data not shown). The TUNEL and CD11b findings agreed well with the clinical evaluations that revealed no significant inflammation in the eyes of the naïve, naked-vector, or *BMP7+HGF* groups (Fig. 2).

Proinflammatory, Profibrotic, and Proangiogenic mRNA Evaluations

The effects of *BMP7+HGF* overexpression at the molecular level in rabbit eyes *in vivo* was appraised by measuring the mRNA levels of proinflammatory (*NFκB*, *TNFα*, and *COX-2*), fibrotic (*αSMA*, *FN*, and *TGFβ1*), and angiogenic (*VEGF*, *PEDF*, and *ANGPT1*) genes in corneas collected after euthanasia at 7 months using qRT-PCR (Fig. 9). The qRT-PCR analysis found no significant variations ($P > 0.05$) in the expression of selected proinflammatory (Fig. 9A), profibrotic (Fig. 9B), or proangiogenic (Fig. 9C) genes in the corneas of the naïve, naked-vector, or *BMP7+HGF* groups. Corneas collected at 2 months showed similar results (data not shown).

Evaluation of Gene Copies

Real-time PCR was used to determine number of copies of *BMP7* and *HGF* genes at 2 months and 7 months. The PCR analysis determined that the *BMP7* and *HGF* gene copies were present in the rabbit corneas throughout the testing period (Fig. 10). At 2 months, the *BMP7* and *HGF* gene copies were $1.38 \times 10^3 \pm 0.62 \times 10^3$ and $2.45 \times 10^2 \pm 0.54 \times 10^3$, respectively, per 1 μg of DNA. At 7 months, the *BMP7* and *HGF* gene copies were $4.56 \times 10^1 \pm 0.71 \times 10^1$ and $1.21 \times 10^1 \pm 0.53 \times 10^1$, respectively, per 1 μg of DNA. An expected gradual decline in *BMP7* and *HGF* gene copies was observed in rabbit corneas (Fig. 10).

BMP7 and *HGF* Gene mRNA Expression

Quantitative RT-PCR was used to measure mRNA expression of *BMP7* and *HGF* genes in rabbit corneas collected at 2 months and 7 months after gene transfer. Amplified *BMP7* and *HGF* mRNA levels were observed in the corneas of the *BMP7+HGF* group ($P < 0.01$) compared with the naïve and naked-vector groups during the course of the study (Fig. 11). At 2 months, the mRNA expression levels of *BMP7* and

Table 2. Modified MacDonald–Shadduck Scoring of Ocular Health Assessment

Groups	Modified MacDonald–Shadduck Cumulative Scores			
	Before Gene Transfer	1 Month After Gene Transfer	3 Months After Gene Transfer	7 Months After Gene Transfer
Naïve	0	0	0	0
Naked-vector	0	0.07 ± 0.03	0.10 ± 0.03	0.10 ± 0.03
<i>BMP7+HGF</i>	0	0.10 ± 0.03	0.10 ± 0.03	0.10 ± 0.03

The cumulative modified MacDonald–Shadduck scores showed that no significant differences were recorded after *BMP7+HGF* gene therapy as compared with the corresponding naïve control and naked-vector control groups. The statistical analyses were performed using two-way ANOVA with the Bonferroni multiple comparison post hoc test. $P > 0.05$ was considered statistically non-significant.

HGF were 3.03 ± 0.15 and 1.92 ± 0.12 , fold higher than naïve group respectively. At 7 months, the mRNA expression levels of *BMP7* and *HGF* were 2.14 ± 0.14 and 1.42 ± 0.13 , fold higher than naïve group respectively.

worldwide.^{1–6} The pathogenesis of corneal fibrosis is a complex cascade of molecular signaling events involving numerous cytokines, growth factors, and ECM remodeling factors. Currently, pharmacologic therapies are commonly used to treat corneal fibrosis despite limitations in efficacy, safety, and tolerability. In 2018, we demonstrated an efficacious inhibition of corneal fibrosis in rabbits *in vivo* with minimal acute toxicity through the use of PEI2-GNP–(*BMP7+HGF*) nanomedicine.²⁴ In the present study, we report the long-term safety and tolerability of

Discussion

Fibrosis after corneal injury is a common cause of visual disability that affects millions of patients

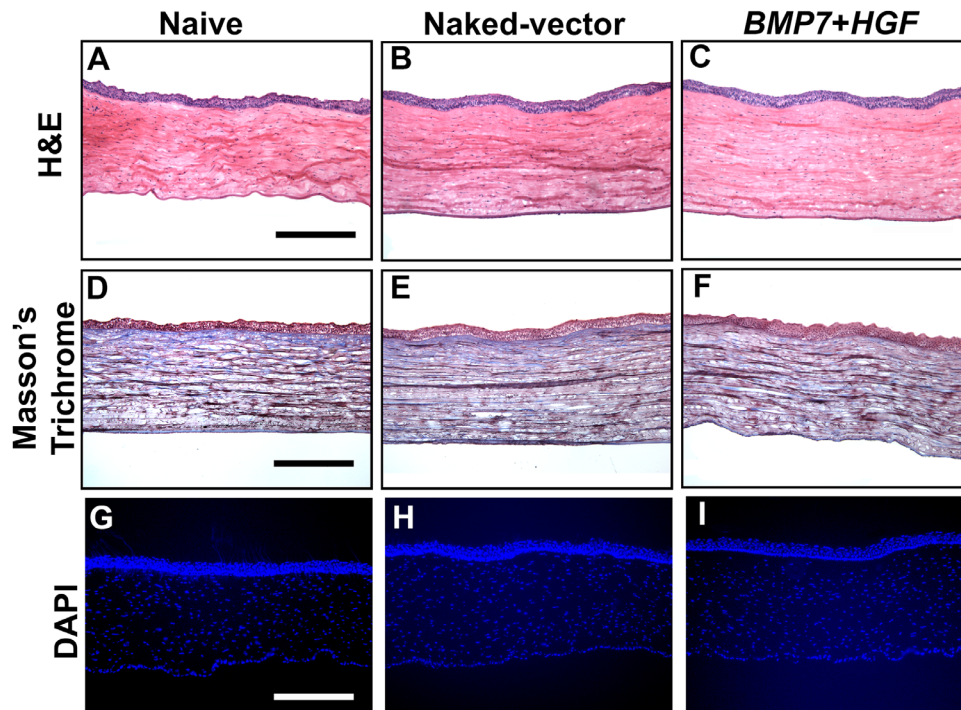


Figure 7. Histological examinations of rabbit corneal tissues showing unremarkable changes in gross morphology, cellular architecture and density, or collagen levels in the naïve, naked-vector, and *BMP7+HGF* groups. The H&E staining (A–C), Masson’s trichrome staining (D–F), and DAPI-nuclear staining (G–I) disclosed the safety and tolerability of *BMP7+HGF* gene therapy to rabbit eyes, as the cellular parameters were comparable to those for the naïve and naked-vector control animals at 7 months. Histological findings at 2 months were similar to those at 7 months (data not shown). Scale bar: 100 µm.

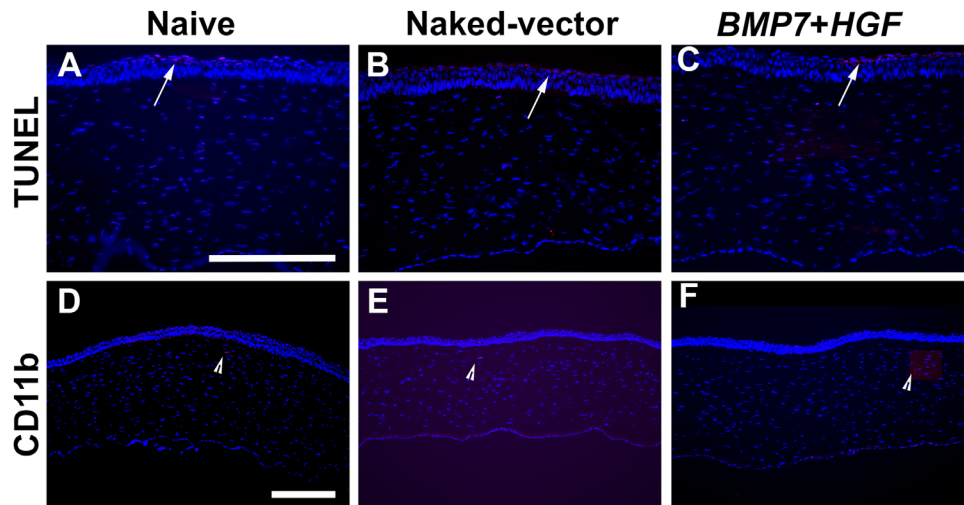


Figure 8. Representative immunofluorescence images of TUNEL apoptosis and CD11b assays showing that *BMP7+HGF* gene therapy is safe, non-toxic, and non-immunogenic to rabbit eyes *in vivo*. The apoptosis assay (A–C) detected occasional TUNEL+ cells in stroma and expected TUNEL+ cells (arrows) in superficial epithelial cells in corneal tissue sections of the naïve, naked-vector, and *BMP7+HGF* groups. Likewise, the CD11b staining (D–F) showed no appreciable presence of inflammatory cells in corneal tissue sections and an expected few CD11b+ cells (arrowhead) in the naïve, naked-vector, and *BMP7+HGF* groups at 7 months. TUNEL assay findings at 2 months were similar to those at 7 months (data not shown). Scale bar: 50 μm (A–C); 100 μm (D–F).

PEI2-GNP–(*BMP7+HGF*) gene therapy in the eye *in vivo* as evaluated through the use of a rabbit model, physical eye examinations, advanced multimodal clinical eye imaging tools, and histological and molecular biological techniques.

The role of *BMP7* and *HGF* genes in the modulation of corneal wound healing is well documented.^{22,24,27} Furthermore, *BMP7* has been shown to regulate many cellular functions, including cell growth, differentiation, fibrosis, and TGF β /Smad signaling, in many organs.^{22,26,34,35} In the eyes of adult animals, endogenous *BMP7* levels are low, and exogenous administration of *BMP7* has shown improved epithelial regeneration and reduced stromal fibrosis in the cornea *in vivo*.^{36,37} Tandon et al.²² reported that *BMP7* in the cornea inhibited myofibroblast and fibrosis formation by regulating Smad signaling. The expression and role of *HGF* in the cornea have been studied by our group and many other investigators. *HGF* is shown to promote corneal epithelial repair, induce apoptosis selectively in corneal myofibroblasts, and suppress ocular inflammation and fibrosis.^{24,38–40} Nonetheless, the long-term beneficial or detrimental consequences of *HGF* and *BMP7* alone or in combination have never been studied previously in the cornea. To the best of our knowledge, this is the first study to explore the long-term safety and tolerability of *BMP7+HGF* gene therapy *in vivo* using a New Zealand White rabbit model and multimodal clinical eye imaging *in situ* for 7 months.

The PEI2-GNP nanoparticle vector has attracted much attention because of its bio-inertness, non-

toxicity, ease of synthesis, and efficient condensation of DNA.^{17,22,24} The topical route of application for PEI2-GNP–(*BMP7+HGF*) gene therapy was chosen because it is the most convenient means of clinically delivering drugs to the eye and largely avoids pharmacokinetic challenges and side-effects associated with systemic administration. Our group has previously demonstrated the efficacy and safety of this topical gene delivery method.^{22,24} Clinical eye examinations performed in a masked manner by at least two independent clinicians or researchers found a lack of toxicity. Specifically, the clinical eye examinations were without signs of ocular toxicity such as altered tear secretion, changes in IOP, corneal edema, opacity, neovascularization, or corneal abrasions. These findings reflect the safety of PEI2-GNP–(*BMP7+HGF*) gene therapy in rabbit eyes *in vivo* (Figs. 1–4). Furthermore, these findings agree well with our previous reports and are supported by other literature related to gene therapy in ocular tissue.^{17,22,24} The confocal microscopy images showed the normal brightened cell boundaries of superficial, wing, and basal cells of epithelial layers; the normal gray amorphous background of keratocyte cells with myelinated nerve fibers visualized at a lower density; and increased thickness in the stromal layers. The single layer of hexagonal-shaped cells appeared with bright cell bodies in the endothelial layer in the gene therapy group and in the corresponding naïve and naked-vector control groups. Collectively, the images of confocal and specular microscopy showed no signs of morphological or pathological alterations at the cellular level in the

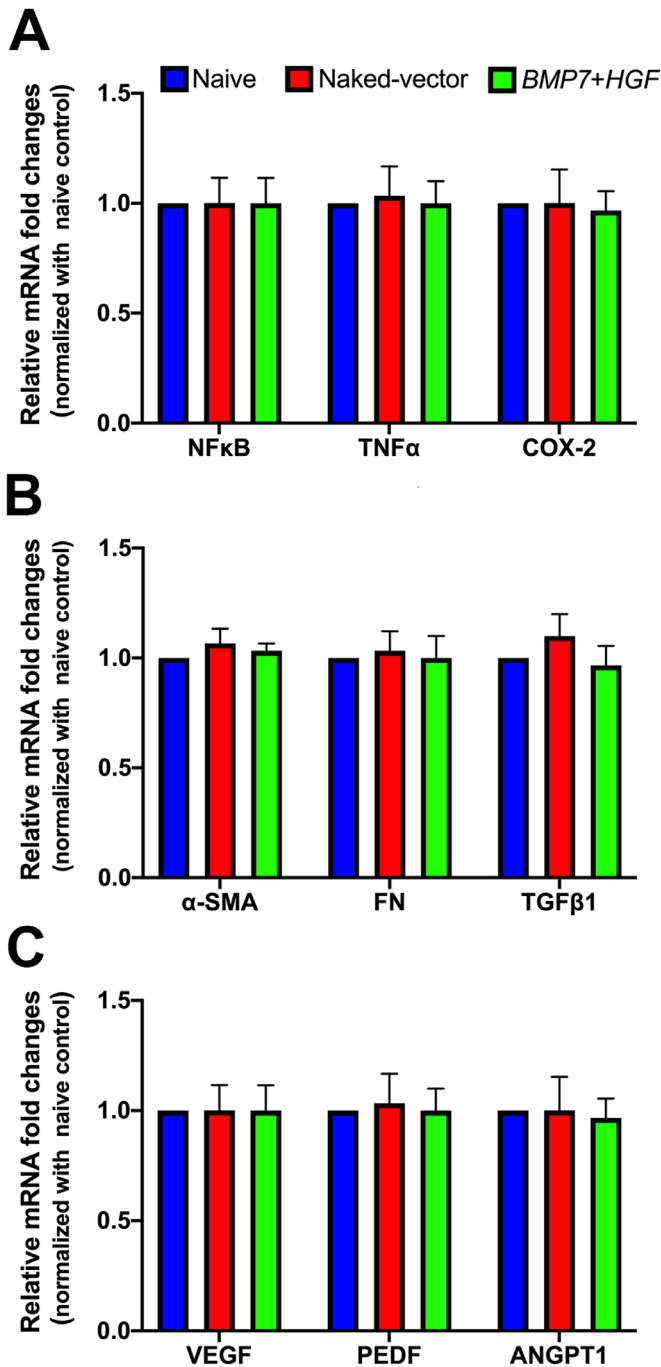


Figure 9. Quantitative RT-PCR analysis of corneal tissues showing mRNA levels of proinflammatory, profibrotic, and proangiogenic genes in naïve, naked-vector, and *BMP7+HGF* groups at 7 months. No significant changes were observed in the expression levels of (A) proinflammatory genes (*NFκB*, *TNFα*, and *COX-2*), (B) profibrotic genes (*α-SMA*, *FN*, and *TGFβ1*), or (C) proangiogenic genes (*VEGF*, *PEDF*, and *ANGPT1*) in the three groups. These data indicate that *BMP7+HGF* gene therapy did not alter gene expression at the molecular level. One-way ANOVA with Tukey post hoc test was used for multiple comparison, and $P > 0.05$ was considered non-significant in statistical analyses. The qRT-PCR findings at 2 months were similar to those at 7 months (data not shown).

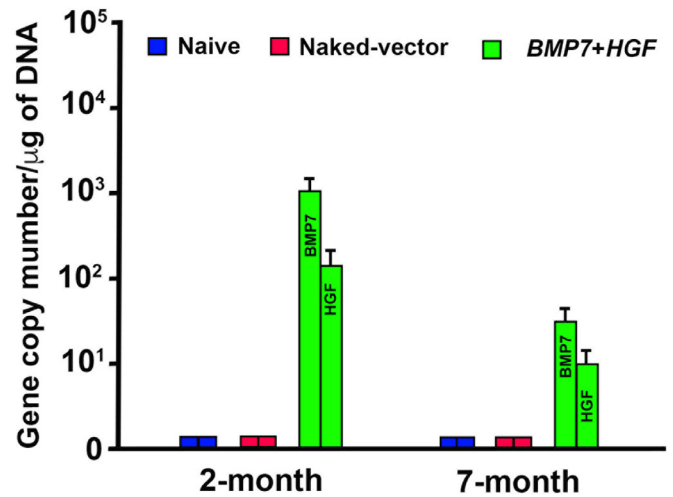


Figure 10. Quantitative RT-PCR analysis measuring numbers of delivered gene copies of *BMP7* and *HGF* in rabbit corneas at 2 months and 7 months. One-way ANOVA with Tukey post hoc test was used for multiple comparison for naïve and naked-vector control group animals. Error bars represent \pm SEM; * $P < 0.05$ against the naïve- and naked-vector control groups was considered significant.

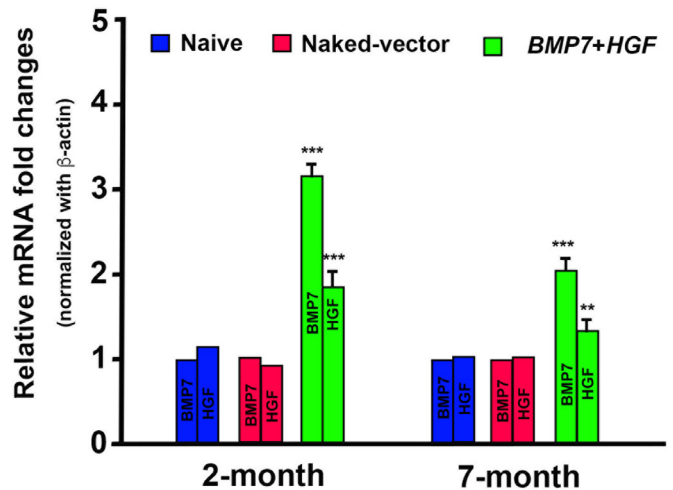


Figure 11. Quantitative RT-PCR analysis measuring mRNA of *BMP7* and *HGF* in naïve, naked-vector, and *BMP7+HGF* groups at 2 months and 7 months. One-way ANOVA with Tukey post hoc test was used for multiple comparison. Error bars represent \pm SEM; ** $P < 0.01$ and *** $P < 0.01$ against the naïve- and naked-vector control groups were considered significant.

treated or control groups (Figs. 5, 6), in agreement with our clinical observations (Figs. 1–3). We performed histological and immunofluorescence evaluations of each group to evaluate them for morphological changes in cellular structure that may indicate toxicity due to gene delivery. Full-thickness corneal sections were evaluated, and histology and fluorescence imaging evaluations of these sections showed no signs of morphological alteration or cellular density in any cell types of corneal tissue sections as compared with

corresponding naïve or naked-vector control group animals (Figs. 7, 8). These findings are in agreement with the clinical and confocal microscopy assessments (Fig. 6). The molecular level assessment showed no significant difference in proinflammatory, profibrotic, or proangiogenic genes in the *BMP7+HGF* group as compared with the naïve or naked-vector control groups (Fig. 9) and did not upset the normal homeostasis balance of cellular cytokines. The molecular analysis data were well aligned with the clinical and histological observations, which also showed no signs of significant changes after *BMP7+HGF* gene therapy in corneal tissues.

The safety and toxicity of the vector and gene constructs for both patients and the environment are major concerns for any gene therapy modality. Our lab has developed expertise in delivering genes into the corneal stroma of rodent and rabbit eyes via a topical method with minimal toxicity using viral and non-viral vectors.^{11–15,17–24} This study supports our earlier corneal gene transfer work through detection of the delivered *BMP7* and *HGF* gene copies (Fig. 10) and mRNA expression (Fig. 11) in rabbit corneas that underwent gene transfer via PEI2-GNP nanoparticles. To the best of our knowledge, this is the first study to show the expression of delivered genes in rabbit cornea via PEI2-GNP nanoparticles over a 7-month period without major adverse effects to the eyes. Additionally, the detection of similar levels of *BMP7* and *HGF* copies at 2 months in rabbit corneas corroborates an earlier report in which levels of these two genes in rabbit cornea were measured at 1 month.²⁴ These data suggest that the level of therapeutic genes introduced via PEI2-GNP nanoparticles in rabbit cornea is retained *in vivo*. One of the limitations of this study is that it employed fewer time points (2 months and 7 months) for histological and molecular investigations. This design prevented identifying the precise time at which a reduction in therapeutic genes began after 2 months during the tested 7 months. Another limitation of the study includes a lack of direct evidence regarding whether the low gene copy numbers and mRNA amounts of *BMP7* and *HGF* genes determined at 7 months are sufficient to deliver functional or therapeutic responses in rabbit cornea *in vivo*. Our future studies will address these weaknesses.

The modified MacDonald–Shadduck cumulative scores (Table 2) indicated that extended nanoparticle-mediated overexpression of *BMP7* and *HGF* genes for 7 months in rabbit cornea did not jeopardize corneal health or induce ocular symptoms *in vivo*. This observation aligns with non-ocular literature reporting no noticeable adverse effects in skin, liver, or skeletal muscles for greater than 12 months after receiving

genes via a non-viral method.^{41,42} Furthermore, *BMP7* and *HGF* overexpression in rabbit cornea did not cause any deviations in animals' weight, water intake, behavioral response, or food intake regimes during the study (data not shown).

In summary, the comprehensive clinical examination, advanced clinical imaging, histological evaluation, and molecular biological techniques showed that PEI2-GNP–(*BMP7+HGF*) gene therapy was safe and well tolerated in rabbit corneal tissue without showing any noticeable adverse effect *in vivo*. We deduce that PEI2-GNP–mediated *BMP7+HGF* gene therapy has bench-to-bedside translational potential for treating corneal fibrosis *in vivo* without significant short- or long-term toxicity to the eye, based on current and earlier reports.²⁴

Acknowledgments

Supported by a Veterans' Health Affairs Merit grant (1I01BX000357 to RRM); by a Research Career Scientist grant (IK6BX005646 to RRM); by grants from the National Eye Institute, National Institutes of Health (5R01EY017294, 5R01EY030774, and 1U01EY031650 to RRM); and by the Ruth Kraeuchi Missouri Endowed Chair Ophthalmology Fund (RRM) at the University of Missouri.

Disclosure: **S. Gupta**, None; **N.R. Sinha**, None; **L.M. Martin**, None; **L.M. Keele**, None; **P.R. Sinha**, None; **J.T. Rodier**, None; **J.R. Landreneau**, None; **N.P. Hesemann**, None; **R.R. Mohan**, None

References

1. Robaei D, Watson S. Corneal blindness: a global problem. *Clin Exp Ophthalmol*. 2014;42(3):213–214.
2. Global Burden of Disease Study 2013 Collaborators. Global, regional, and national incidence, prevalence, and years lived with disability for 301 acute and chronic diseases and injuries in 188 countries, 1990–2013: a systematic analysis for the Global Burden of Disease Study 2013. *Lancet*. 2015;386(9995):743–800.
3. Barrientes B, Nicholas SE, Whelchel A, Sharif R, Hjortdal J, Karamichos D. Corneal injury: clinical and molecular aspects. *Exp Eye Res*. 2019;186:107709.
4. Friedlander M. Fibrosis and diseases of the eye. *J Clin Invest*. 2007;117(3):576–586.

5. Menko AS, Walker JL, Stepp MA. Fibrosis: shared lessons from the lens and cornea. *Anat Rec (Hoboken)*. 2020;303(6):1689–1702.
6. Farid M, Rhee MK, Akpek EK, et al. Corneal edema and opacification preferred practice pattern. *Ophthalmology*. 2019;126(1):P216–P285.
7. Goswami R, Subramanian G, Silayeva L, et al. Gene therapy leaves a vicious cycle. *Front Oncol*. 2019;9:297–297.
8. Mathews PM, Lindsley K, Aldave AJ, Akpek EK. Etiology of global corneal blindness and current practices of corneal transplantation: a focused review. *Cornea*. 2018;37(9):1198–1203.
9. Margo JA, Munir WM. Corneal haze following refractive surgery: a review of pathophysiology, incidence, prevention, and treatment. *Int Ophthalmol Clin*. 2016;56(2):111–125.
10. Wilson SL, El Haj AJ, Yang Y. Control of scar tissue formation in the cornea: strategies in clinical and corneal tissue engineering. *J Funct Biomater*. 2012;3(3):642–687.
11. Mohan RR, Sinha S, Tandon A, Gupta R, Tovey JC, Sharma A. Efficacious and safe tissue-selective controlled gene therapy approaches for the cornea. *PLoS One*. 2011;6(4):e18771.
12. Mohan RR, Sharma A, Cebulko TC, Tandon A. Vector delivery technique affects gene transfer in the cornea *in vivo*. *Mol Vis*. 2010;16:2494–2501.
13. Mohan RR, Sharma A, Netto MV, Sinha S, Wilson SE. Gene therapy in the cornea. *Prog Retin Eye Res*. 2005;24(5):537–559.
14. Mohan RR, Rodier JT, Sharma A. Corneal gene therapy: basic science and translational prospective. *Ocular Surf*. 2013;11(3):150–164.
15. Mohan RR, Schultz GS, Hong J-W, Mohan RR, Wilson SE. Gene transfer into rabbit keratocytes using AAV and lipid-mediated plasmid DNA vectors with a lamellar flap for stromal access. *Exp Eye Res*. 2003;76(3):373–383.
16. Bastola P, Song L, Gilger BC, Hirsch ML. Adeno-associated virus mediated gene therapy for corneal diseases. *Pharmaceutics*. 2020;12(8):767.
17. Sharma A, Tandon A, Tovey JCK, et al. Polyethylenimine-conjugated gold nanoparticles: gene transfer potential and low toxicity in the cornea. *Nanomedicine*. 2011;7(4):505–513.
18. Rodier JT, Tripathi R, Fink MK, et al. Linear polyethylenimine-DNA nano-construct for corneal gene delivery. *J Ocul Pharmacol Ther*. 2019;35(1):23–31.
19. Donnelly KS, Giuliano EA, Sharma A, Tandon A, Rodier JT, Mohan RR. Decorin-PEI nanoconstruct attenuates equine corneal fibroblast differentiation. *Vet Ophthalmol*. 2014;17(3):162–169.
20. Mohan RR, Tandon A, Sharma A, Cowden JW, Tovey JC. Significant inhibition of corneal scarring *in vivo* with tissue selective, targeted AAV5 decorin gene therapy. *Invest Ophthalmol Vis Sci*. 2011;52(7):4833–4841.
21. Mohan RR, Tovey JCK, Sharma A, Schultz GS, Cowden JW, Tandon A. Targeted decorin gene therapy delivered with adeno-associated virus effectively retards corneal neovascularization *in vivo*. *PLoS One*. 2011;6(10):e26432.
22. Tandon A, Sharma A, Rodier JT, Klibanov AM, Rieger FG, Mohan RR. BMP7 gene transfer via gold nanoparticles into stroma inhibits corneal fibrosis *in vivo*. *PLoS One*. 2013;8(6):e66434.
23. Gupta S, Rodier JT, Sharma A, et al. Targeted AAV5-Smad7 gene therapy inhibits corneal scarring *in vivo*. *PLoS One*. 2017;12(3):1–18.
24. Gupta S, Fink MK, Ghosh A, et al. Novel combination BMP7 and HGF gene therapy instigates selective myofibroblast apoptosis and reduces corneal haze *in vivo*. *Invest Ophthalmol Vis Sci*. 2018;59(2):1045–1057.
25. Rothe M, Schambach A, Biasco L. Safety of gene therapy: new insights to a puzzling case. *Curr Gene Ther*. 2014;14(6):429–436.
26. Tandon A, Tovey JCK, Sharma A, Gupta R, Mohan RR. Role of transforming growth factor-beta in corneal function, biology, and pathology. *Curr Mol Med*. 2010;10(6):565–578.
27. Wilson SE, Chen L, Mohan RR, Liang Q, Liu J. Expression of HGF, KGF, EGF, and receptor messenger RNAs following corneal epithelial wounding. *Exp Eye Res*. 1999;68:377–397.
28. Thomas M, Klibanov AM. Conjugation to gold nanoparticles enhances polyethylenimine's transfer of plasmid DNA into mammalian cells. *Proc Natl Acad Sci USA*. 2003;100(16):9138–9143.
29. Altmann S, Emanuel A, Toomey M, et al. A quantitative rabbit model of vaccinia keratitis. *Invest Ophthalmol Vis Sci*. 2010;51(9):4531–4540.
30. Zyablitskaya M, Jayyosi C, Takaoka A, et al. Topical corneal cross linking solution delivered via corneal reservoir in Dutch-Belted rabbits. *Transl Vis Sci Technol*. 2020;11(9):20.
31. Huang J, Maram J, Tepelus TC, et al. Comparison of manual & automated analysis methods for corneal endothelial cell density measurements by specular microscopy. *J Optom*. 2018;11(3):182–191.
32. Gupta S, Fink MK, Martin LM, et al. A rabbit model for evaluating ocular damage from acrolein toxicity *in vivo*. *Ann N Y Acad Sci*. 2020;1480(1):233–245.

33. Tanaka T. Leukocyte adhesion molecules. In: Ratcliffe MJH, ed. *Encyclopedia of Immunobiology*. Cambridge, MA: Academic Press; 2016;505–511.
34. Zou GL, Zuo S, Lu S, et al. Bone morphogenetic protein-7 represses hepatic stellate cell activation and liver fibrosis via regulation of TGF- β /Smad signaling pathway. *World J Gastroenterol*. 2019;25(30):4222–4234.
35. Weiskirchen R, Meurer SK, Gressner OA, et al. BMP-7 as antagonist of organ fibrosis. *Front Biosci (Landmark Ed)*. 2009;14:4992–5012.
36. Kowtharapu BS, Prakasam RK, Murin R, et al. Role of bone morphogenetic protein 7 (BMP7) in the modulation of corneal stromal and epithelial cell functions. *Int J Mol Sci*. 2018;19(5):1415.
37. Saika S, Ikeda K, Yamanaka O, et al. Therapeutic effects of adenoviral gene transfer of bone morphogenetic protein-7 on a corneal alkali injury model in mice. *Lab Invest*. 2005;85(4):474–486.
38. Miyagi H, Thomasy SM, Russell P, Murphy CJ. The role of hepatocyte growth factor in corneal wound healing. *Exp Eye Res*. 2018;166:49–55.
39. Omoto M, Suri K, Amouzegar A, et al. Hepatocyte growth factor suppresses inflammation and promotes epithelium repair in corneal injury. *Mol Ther*. 2017;25(8):1881–1888.
40. de Oliveira RC, Murillo S, Saikia P, et al. The efficacy of topical HGF on corneal fibrosis and epithelial healing after scar producing PRK injury in rabbits. *Transl Vis Sci Technol*. 2020;9(4):29.
41. Gothelf A, Eriksen J, Hojman P, et al. Duration and level of transgene expression after gene electrotransfer to skin in mice. *Gene Ther*. 2010;17(7):839–845.
42. Muramatsu T, Arakawa S, Fukazawa K, et al. *In vivo* gene electroporation in skeletal muscle with special reference to the duration of gene expression. *Int J Mol Med*. 2001;7(1):37–42.